Compositional changes of Pd-Au bimetallic nanoclusters upon hydrogenation

M. Di Vece,[1] S. Bals,[2] J. Verbeeck,[2] P. Lievens,[1] and G. Van Tendeloo[2]
[1]*Laboratorium voor Vaste-Stoffysica en Magnetisme and Institute for Nanoscale Physics and Chemistry (INPAC), K. U. Leuven, B-3001 Leuven, Belgium*
[2]*EMAT, University of Antwerp, Groenenborgerlaan 171, B-2020 Antwerp, Belgium*
(Received 19 May 2009; revised manuscript received 4 August 2009; published 21 September 2009)

Changes in the size distribution and composition of bimetallic Pd-Au nanoclusters have been observed after hydrogen exposure. This effect is caused by hydrogen-induced Ostwald ripening whereby the hydrogen reduces the binding energy of the cluster atoms leading to their detachment from the cluster. The composition changes due to a difference in mobility of the detached palladium and gold atoms on the surface. Fast palladium atoms contribute to the formation of larger nanoclusters, while the slower gold atoms are confined to the smaller nanoclusters. These transformations in the Pd-Au nanocluster size and composition set a limit for chemical reactions in which such nanoclusters are involved together with hydrogen.

DOI: 10.1103/PhysRevB.80.125420 PACS number(s): 61.46.Bc, 61.66.Dk, 68.35.Dv, 68.37.Lp

I. INTRODUCTION

The investigation of nanoclusters with respect to their interaction with other substances is particularly interesting from a catalytic point of view.[1] Both single element[2] and bimetallic[3] nanoclusters have interesting catalytic properties, which are of great value to industry.[4] For example, gold-palladium nanoparticles on TiO_2 have an extremely high-turnover rate for the oxidation of aldehydes to alcohols.[5] As many catalytic processes are performed at elevated temperatures, the stability of such nanoscale catalysts determines the efficiency. High temperatures enhance oxidation, and nanoclusters on surfaces are changing size due to Ostwald ripening[6] in which the larger clusters take up mobile atoms at the expense of smaller clusters.[7] However, this phenomenon is not restricted to high temperatures alone but can also be observed by exposing palladium nanoclusters to hydrogen.[8] Hydrogen-induced Ostwald ripening is the result of a decreasing sublimation energy upon hydrogenation, which stimulates the detachment of atoms from the clusters at room temperature. This raises the question of how hydrogen would influence a bimetallic hydrogen absorbing nanocluster. The palladium-gold alloy is of main importance in catalysis[9,10] and since palladium absorbs hydrogen, effects can be expected upon hydrogenation. Calculations demonstrate the occurrence of structural transformations at high temperatures for Pd-Au bimetallic nanoclusters.[11] Therefore, it is very possible that hydrogen would also induce similar changes. As hydrogen is involved in many catalytic processes, its influence on the catalyst is of major practical importance.

Nanoscale objects are now routinely investigated by transmission electron microscopy (TEM). In a recent study, high-angle annular dark-field (HAADF) scanning transmission electron microscopy (STEM) was used to determine the number of atoms in a nanocluster.[12] This could be done since the HAADF-STEM signal depends on the number of atoms in a column. Furthermore, the signal is also sensitive to the difference in atomic number, which is called *Z*-sensitivity. This *Z*-sensitivity can also be used to distinguish between different elements in nanoclusters[13] allowing the compositional determination from the HAADF intensity alone.

In this paper the effect of hydrogen on Pd-Au bimetallic nanoclusters is investigated using HAADF STEM. The nanocluster diameter and HAADF intensity were statistically analyzed to study morphological as well as compositional changes under the influence of hydrogen exposure. The mobility of the detached atoms on the surface is used to explain the experimental results.

II. EXPERIMENTAL

A dual-target dual-laser vaporization source[14–16] was used to prepare the Pd-Au bimetallic and pure Au nanoclusters. The nanoclusters were deposited[17,18] on TEM grids, which consist of amorphous carbon layers on a lacy polymer film supported by a Cu grid. The ratio between palladium and gold for the bimetallic nanoclusters was controlled by measuring the flux of both single metals. To maintain the hydrogen absorption capacity the palladium contribution was set to 76%, leaving gold, which does not absorb hydrogen, to 24%. Half of the identical samples were exposed to hydrogen at 1 bar for 2 h. Before introducing hydrogen into the cell containing the TEM grids with nanoclusters, a vacuum of 10^{-1} mbar was introduced to remove most of the air. All of these procedures were performed at room temperature.

The samples have been studied with HAADF-STEM on a JEOL 3000F (inner HAADF detector angle 60 mrad). In this technique, the illumination is focused to a probe of approximately 0.2 nm, which is scanned across the sample, resulting in an image representing the scattering power onto the HAADF detector. The intensity associated with a HAADF-STEM image is in a first approximation proportional to Z^2, where Z is the average atomic number projected along the beam direction and the thickness of the column. This makes a direct interpretation of HAADF-STEM images relatively straightforward since changes in thickness and average atomic number are directly visible in the image intensity.

III. RESULTS AND DISCUSSION

In Fig. 1, a HAADF STEM image of the hydrogenated Pd-Au nanoclusters is shown. A wide variety of nanocluster

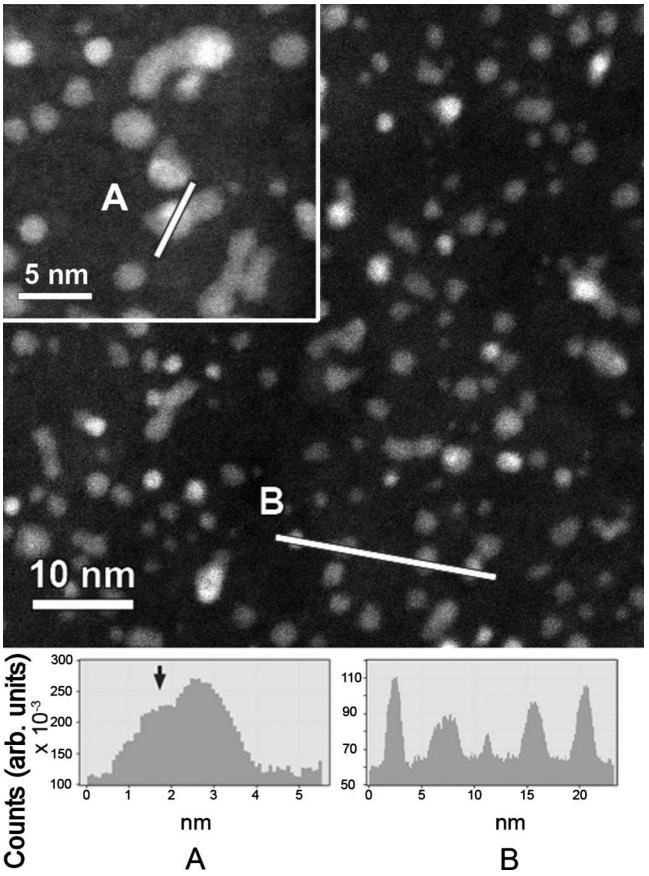

FIG. 1. A STEM image of hydrogenated Pd-Au nanoclusters with (A) a profile of a core-shell nanocluster with gold as the core and (B) a profile of several clusters, indicating a range of Pd/Au compositions.

sizes and shapes are present. Most of the nanoclusters have a round profile in accordance with the gas-phase creation. Some clusters however have a more elongated shape; this is likely the result of a collision of individual clusters at the surface during deposition. Some of the largest nanoclusters have a bright spot within a shell of a somewhat lower intensity. The HAADF profile of such a nanocluster is shown in Fig. 1(A) and clearly shows a discontinuity at the border, indicating a discrete intensity step. Since the HAADF intensity is proportional to the atomic mass and the atomic numbers of palladium and gold are 46 and 79, respectively, this significant HAADF STEM intensity step can be explained by a different composition. The high-intensity core therefore corresponds to gold while the about four times darker shell corresponds to palladium. In general the composition of the core and shell depends on the bimetallic ratio and the temperature.[11] The core-shell structure with a gold core and palladium shell has been observed before[19] for a 1:1 concentration. However, the majority of the nanoclusters in Fig. 1(A) does not show such a discrete boundary but a more homogeneous gray value.[20] Additionally, many nanoclusters of similar size have different HAADF intensities. A HAADF profile of a representative collection is given in Fig. 1(B). The nanocluster at the left with a small diameter, has an almost two times higher HAADF intensity as compared to

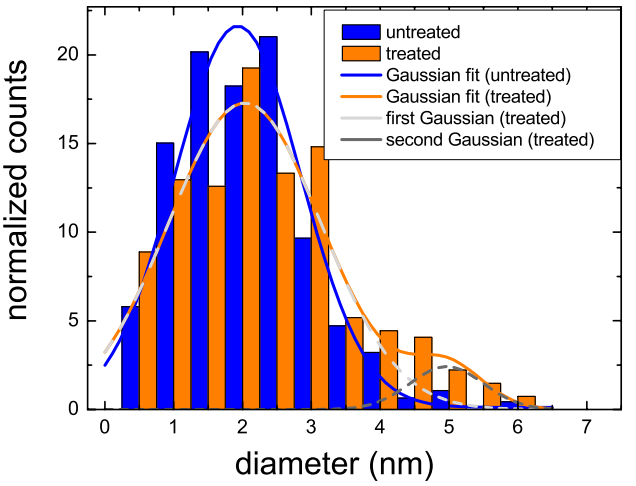

FIG. 2. (Color online) Nanocluster size (diameter) distribution as obtained from the STEM images. The number of counted nanoclusters are 466 and 270 for the untreated and treated Pd-Au nanoclusters, respectively. The distributions are normalized to 20 and fitted with a single and double Gaussian for the as-deposited (R^2=0.96) and treated (R^2=0.90) nanoclusters, respectively.

the nanoclusters with larger diameters. Assuming a spherical shape for both clusters, the difference in intensity is likely to be due to alloying, in which the Au/Pd ratio determines the resulting HAADF intensity.

HAADF-STEM images of the as-deposited sample are not shown, since differences with the images of the hydrogenated nanoclusters are difficult to observe by the naked eye. However, statistical analysis provided significant differences between the images of the as-deposited and the hydrogenated samples. Size distribution analysis is performed by threshold masking the particles and subtracting a constant background from the carbon layer. Particle size and average intensity are obtained for many particles from a large number of HAADF images and a size distribution for the hydrogenated and as-deposited samples is shown in Fig. 2, illustrating the differences between both. The size distribution of the as-deposited nanoclusters is similar to that of gold nanoclusters deposited from the same cluster source on MgO (Ref. 21) with a mean diameter of about 2.5 nm. This is in agreement with the various parameters used in the formation of nanoclusters such as the specific material, ablation laser intensity, cooling gas pressure, temperature, and nozzle shape. The distributions are fitted with a single and double Gaussian function for the as-deposited and treated nanoclusters, respectively. Introducing a second Gaussian peak at around 5 nm for the as-deposited nanoclusters did not converge during fitting. The position of the main peak shifts from 1.93 (0.06) to 2.0 (0.1) nm while the width increases from 1.8 (0.2) to 2.2 (0.3) nm upon hydrogenation. After hydrogenation the number of nanoclusters smaller than 3 nm is reduced while the number of larger nanoclusters has increased. The second Gaussian peak in the fit of the treated nanoclusters distribution at 5.0 nm contributes significantly. Since the nanoclusters are clearly isolated from each other, a detachment and subsequent movement of nanocluster atoms from one nanocluster to the other is required. Therefore this change in size

distribution can only be the result of hydrogen-induced Ostwald ripening. The palladium and gold atoms must have moved freely over the amorphous carbon layer. A sharp peak around 2 nm remains after hydrogenation, indicating a particular stable size. Combined with the tendency to form larger particles, this suggests a drive toward a bimodal size distribution, which has been observed before for palladium nanoclusters on a TiO_2 substrate.[6]

The palladium concentration and distribution, i.e., core-shell or solid state solution, influences the response to hydrogenation considerably. Hydrogen can only be absorbed if the nanocluster contains enough palladium because gold does not absorb hydrogen. If the palladium is buried deep inside the cluster then the gold layer prevents absorption and subsequent detachment. However, in the case of a palladium shell and a solid solution with sufficient palladium, hydrogen has enough possibilities to stimulate the detachment of metal atoms.

To investigate compositional changes of the Pd-Au nanoclusters during hydrogenation, the integrated HAADF intensity in a particle is plotted as a function of the particle volume (diameter^3) in Fig. 3, assuming spherically shaped particles. As a reference, also a sample consisting of pure gold nanoparticles was investigated. If spherical shaped particles are assumed, a proportionality between diameter and total intensity is expected since the total intensity is related to the total amount of atoms in the particle. Indeed, a linear relation for size selected gold nanoclusters has been observed before in such diagrams.[12,22]

The integrated HAADF intensity of the nanoclusters as a function of the volume in Fig. 3(A) shows that a wide range of integrated HAADF values are present for each diameter. These distributions are confined in a triangular space, which is indicated by two base lines, which are drawn as guide for the eye at the borders of the distribution. The difference in slope of about 3.4 agrees well with the ratio of the square of the atomic numbers of palladium (106.4) and gold (197.0) ($Z^2_{Pd}/Z^2_{Au}=3.4$).

As the HAADF STEM images of the gold nanoclusters are not recorded under identical conditions, the HAADF intensity needs rescaling toward the corresponding gold values in Figs. 3(A) and 3(B). The average slope of the experimental gold values was fitted onto the gold baseline.

In Fig. 3(A) the larger gold nanoclusters have a lower integrated HAADF intensity as compared to the calculated integrated HAADF vs volume relation (upper limit line). This results in a curvature starting from about 40 nm^3 and can be explained by a flattening of the larger nanoclusters. For flat nanoclusters the integrated HAADF value with respect to the lateral diameter is smaller than for the assumed spherical nanoclusters. Partial flattening of the nanoclusters likely occurs during landing as the deposition energy (0.5 eV/atom) was not entirely in the soft-landing regime. The variation in the composition can be another source for a varying HAADF intensity.

In Fig. 3(B) the integrated HAADF intensity is shown up to 40 nm^3. For this shorter range, the gold nanocluster integrated HAADF intensities are distributed around a straight line. The error is the square root of the calculated variance of the data with respect to the fitted line, and indicates the degree of deviation from the straight line. This error, i.e., the deviation of the data points from this straight line, can be interpreted as a measure of the variation in flattening that occurs upon nanocluster impact with the used cluster source.

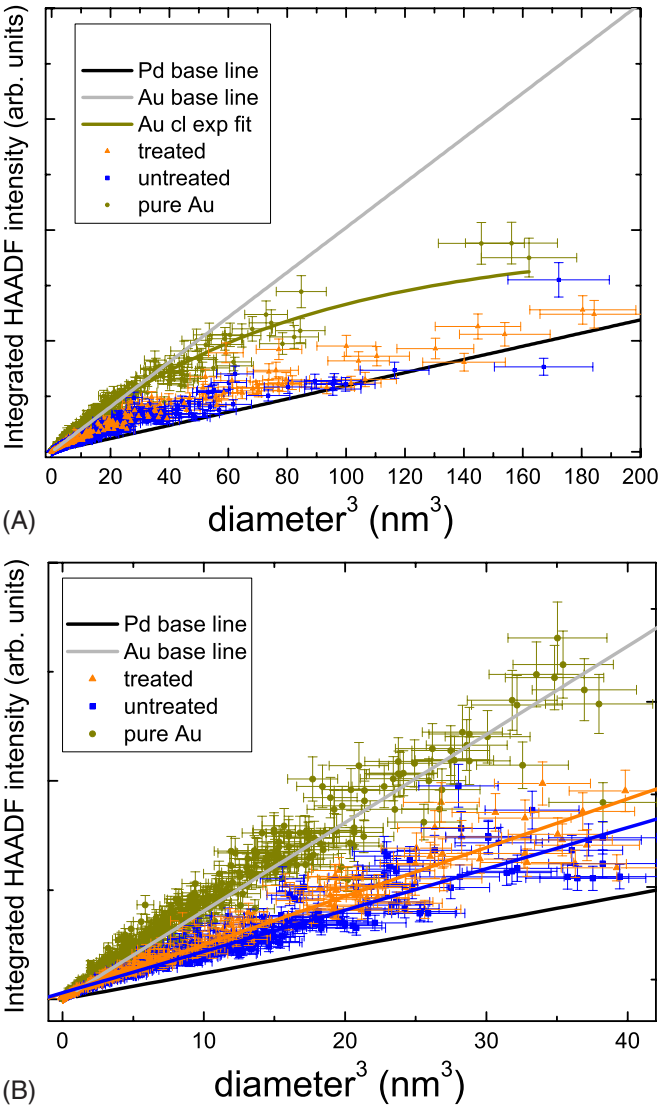

FIG. 3. (Color online) The integrated HAADF intensity as a function of the Pd-Au and Au nanocluster volume for (A) the larger and (B) the small nanoclusters. The black lower curve represents the pure palladium nanocluster values while the gray line represents the pure gold nanoclusters. The curved line in (A) is an exponential decay fit of the pure gold nanoclusters to indicate its relatively decreasing HAADF intensity as a function of diameter. The second and third curves from below in (B) are the fit of the Pd-Au nanocluster data points before ($R^2=0.90$, slope 9463 ± 150) and after ($R^2=0.94$, slope 11123 ± 190) hydrogenation, respectively.

The integrated HAADF intensity of the smaller (diameter$^3<30$ nm^3) pristine and hydrogenated Pd-Au nanoclusters covers the space between the Pd and Au-base lines [Fig. 3(A)]. This corresponds with a large variety in composition extending from pure palladium to pure gold nanoclusters. In contrast, the integrated HAADF intensity of the pristine and hydrogenated larger Pd-Au nanoclusters are closer to the Pd-base line. Clearly already during the nano-

clusters formation the larger nanoclusters contain more palladium, which is in line with thermodynamic considerations.

In Fig. 3(A) the larger Pd-Au nanoclusters are mainly produced after hydrogenation as they remain closer to the palladium base line. Therefore, it is likely that these larger Pd-Au nanoclusters have a higher palladium concentration. Since it is improbable that hydrogenation flattens the nanoclusters, a lower integrated HAADF intensity must correspond to a higher palladium concentration. In general wetting for comparable nanoclusters has not been observed before,[12,22] a change in shape is unlikely to occur and therefore not a source of deviation.

Linear fits of the Pd-Au nanocluster data points before and after hydrogenation in Fig. 3(B) (third and second curves from below, in the range up to 40 nm^3) show a 18% increase in the slope from 9463 ± 150 to 11123 ± 190, respectively. This indicates that after hydrogenation the smaller nanoclusters have a higher gold content (from 24 to $38 \pm 2\%$).

A clear distinction between the small and large Pd-Au nanoclusters after hydrogenation suggests a preferential growth process. During the process of Ostwald ripening, the difference of mobility between palladium and gold ad-atoms are important parameters, which determine the final composition. Palladium atoms have a higher mobility than gold atoms on highly ordered pyrolytic graphite (HOPG).[23] A similar difference in mobility on amorphous carbon could explain the decrease/increase in the average integrated HAADF intensity for the larger/smaller nanoclusters. The gold atoms stay at, or in the vicinity of, the nanocluster while the palladium atoms depart and travel to the larger nanoclusters. Therefore, as the smaller nanoclusters lose palladium leading to a higher gold concentration, they have a somewhat higher integrated HAADF intensity. The larger nanoclusters accumulate palladium atoms due to preferential sticking as the result of Ostwald ripening and have a relatively lower integrated HAADF intensity. The Ostwald ripening process also explains the increased error on the HAADF vs volume slope. The palladium and gold atoms are reshuffled whereby the disorder increases. As the amount of gold determines the hydrogen absorption, it is very likely that the hydrogen absorption and following Ostwald ripening process stops approximately at a gold concentration of $38 \pm 2\%$.

IV. CONCLUSION

In conclusion, hydrogenation of Pd-Au bimetallic nanoclusters results in hydrogen-induced Ostwald ripening by which the size distribution and composition of the nanoclusters change. After hydrogenation the smaller nanoclusters contain more gold while the larger nanoclusters contain more palladium. This is caused by a difference in the surface mobility of the detached atoms: fast palladium atoms form large nanoclusters while the slow gold atoms are left to the small nanoclusters. This phenomenon has important consequences for catalytic reactions, in which bimetallic nanoclusters are involved together with hydrogen. The integrity of hydrogen absorbing catalysts may be lost upon exposure to hydrogen.

ACKNOWLEDGMENT

This work was financially supported by the Fund for Scientific Research—Flanders (FWO), the Flemish Concerted Action (GOA), and the Belgian Federal Interuniversity Attraction Poles (Grant No. IAP/VI/42) Research Programs. S.B., J.V., and G.V.T. acknowledge financial support from the European Union under the Framework 6 program for Integrated Infrastructure Initiative, Reference No. 026019 ESTEEM.

[1] *Nanocatalysis*, edited by U. Heiz and U. Landman (Springer, Berlin, Heidelberg, New York, 2007).
[2] M. Valden, X. Lai, and D. W. Goodman, Science **281**, 1647 (1998).
[3] N. Toshima and T. Yonezawa, New J. Chem. **22**, 1179 (1998).
[4] C. L. Hill and C. M. Prosser-McCartha, Coord. Chem. Rev. **143**, 407 (1995).
[5] D. I. Enache, J. K. Edwards, P. S. Landon, B. Solsona-Espriu, A. F. Carley, A. A. Herzing, M. Watanabe, C. J. Kiely, D. W. Knight, and G. J. Hutchings, Science **311**, 362 (2006).
[6] W. Ostwald, Z. Phys. Chem. (Leipzig) **34**, 495 (1900).
[7] A. Howard, C. E. J. Mittchell, and R. G. Egdell, Surf. Sci. **515**, L504 (2002).
[8] M. Di Vece, D. Grandjean, M. J. Van Bael, C. P. Romero, X. Wang, S. Decoster, A. Vantomme, and P. Lievens, Phys. Rev. Lett. **100**, 236105 (2008).
[9] M. Chen, D. Kumar, C.-W. Yi, and D. W. Goodman, Science **310**, 291 (2005).
[10] M. Bonarowska, J. Pielaszek, V. A. Semikolenov, and Z. Karpiński, J. Catal. **209**, 528 (2002).
[11] H. B. Liu, U. Pal, R. Perez, and J. A. Ascencio, J. Phys. Chem. B **110**, 5191 (2006).
[12] Z. Y. Li, N. P. Young, M. Di Vece, S. Palomba, R. E. Palmer, A. Bleloch, B. C. Curley, R. L. Johnston, J. Jiang, and J. Yuan, Nature (London) **451**, 46 (2008).
[13] M. Di Vece, N. Young, Z. Y. Li, Y. Chen, and R. E. Palmer, Small **2**, 1270 (2006).
[14] W. Bouwen, P. Thoen, F. Vanhoutte, S. Bouckaert, F. Despa, H. Weidele, R. E. Silverans, and P. Lievens, Rev. Sci. Instrum. **71**, 54 (2000).
[15] P. Milani and W. A. deHeer, Rev. Sci. Instrum. **61**, 1835 (1990).
[16] K. Hoshino, T. Naganuma, Y. Yamada, K. Watanabe, A. Nakajima, and K. Kaya, J. Chem. Phys. **97**, 3803 (1992).
[17] H. Hövel, S. Fritz, A. Hilger, U. Kreibig, and M. Vollmer, Phys. Rev. B **48**, 18178 (1993).
[18] C. Binns, Surf. Sci. Rep. **44**, 1 (2001).
[19] T. Akita, T. Hiroki, S. Tanaka, T. Kojima, M. Kohyama, A. Iwase, and F. Hori, Catal. Today **131**, 90 (2008).
[20] E. Pérez-Tijerina, M. G. Pinilla, S. Mejía-Rosales, U. Ortiz-Méndez, A. Torres and M. José -Yacamán, Faraday Discuss. **138**, 353 (2008).
[21] B. Pauwels, G. Van Tendeloo, E. Zhurkin, M. Hou, G. Verschoren, L. T. Kuhn, W. Bouwen, and P. Lievens, Phys. Rev. B **63**, 165406 (2001).
[22] N. P. Young, Z. Y. Li, Y. Chen, S. Palomba, M. Di Vece, and R. E. Palmer, Phys. Rev. Lett. **101**, 246103 (2008).
[23] R. Anton, Phys. Rev. B **70**, 245405 (2004).